

Generation of N -atom W -class states in spatially separated cavities

Mei Lu¹, Yan Xia^{1,*}, Jie Song², and Nguyen Ba An^{3,†}

¹*Department of Physics, Fuzhou University, Fuzhou 350002, China*

²*Department of Physics, Harbin Institute of Technology, Harbin, Heilongjiang 150001, China*

³*Center for Theoretical Physics, Institute of Physics, 10 Dao Tan, Hanoi, Vietnam*

We propose a feasible and efficient scheme to generate N -atom W -class states in spatially separated cavities without using any classical driving pulses. We adopt the model in which the couplings between different atoms are mediated only by virtual excitations of the cavity and fiber fields, so the scheme is insensitive to the cavity decay and fiber photon leakage. We carry out both theoretical investigation in a decoherence-free subspace and numerical calculation accounting for decoherence due to the atomic spontaneous emission as well as the decay of cavity and fiber modes. The theoretical and numerical results agree in the large atom-cavity detuning regime. Our scheme proves to be useful in scalable distributed quantum networks.

I. INTRODUCTION

Entanglement, a fundamental feature in quantum mechanics, is a key resource for quantum information processing (QIP) [1, 2], such as quantum teleportation [3], quantum dense coding [4], quantum cryptography [5] and quantum computation [6]. If a composite system is entangled, the whole system cannot be split into independent subsystems. Typical entangled states are the Bell states [7], the Greenberger-Horne-Zeilinger-class states [8, 9] and the W -class states [10]. A state is called an N -qubit W -class state if it is of the form $x_1|10\cdots 0\rangle + x_2|01\cdots 0\rangle + \cdots + x_N|00\cdots 1\rangle$ with $\sum_{n=1}^N |x_n|^2 = 1$ and $|0\rangle, |1\rangle$ being two orthonormal vectors in the two-dimensional Hilbert space of the qubit. The N -qubit W state corresponds to $x_1 = x_2 = \cdots = x_N = 1/\sqrt{N}$. Compared with other types of entangled states, W -class state constitutes a very important family of states possessing a high

* E-mail: xia-208@163.com

† E-mail: nban@iop.vast.ac.vn

degree of robustness against the qubit loss as they maintain some entanglement when more than two qubits remained [11, 12]. Furthermore, deterministic protocols for teleportation and superdense coding [13] have been designed by utilizing W -class entanglements [19]. An asymmetrical N -partite W -class state is also an essential quantum channel for quantum information splitting [14, 15] and can be converted to another N -partite W -class state via local operations and classical communications [16]. Therefore, the generation of N -partite W -class states has proved to be an urgent task for the QIP.

However, to our knowledge, there are few studies for the given operationally experimental configurations with multipartite entanglement classes. Bastin *et al.* proposed an experimental setup to produce arbitrary symmetric long-lived multiqubit W states in the internal ground levels of photon emitters [17]. An and Wang *et al.* presented protocols to generate N -party W -class states in a single optical microcavity [18, 19]. The W -class states in the above protocols are generated locally. For the distributed QIP, Pellizzari [20] first suggested a scheme to realize the reliable transfer of quantum information between two distant cavities connected by an optical fiber in 1997, providing an effective tool for long-distant quantum communication schemes in recent years [21–26]. Here, by using a single-mode integrated optical $1 \times N$ star coupler [27, 29? ?], we propose a scheme to generate N -atom W -class states in a distributed network, which is nonlocally correlative [28] even in the presence of noise. Another distinct feature of our scheme is that all the bosonic field modes are only virtually populated to overcome the decoherence caused by cavity decays and fiber photon leakages. The excitation exchange among the atoms is caused by the dispersive coupling between the atoms and multiple delocalized bosonic field modes. Therefore, the atom-fiber-cavity system reduces to an effective model that couples only the atomic states while suppresses the states containing real bosonic modes. In addition, no classical pulses are needed so that the scheme is easy to operate. All these features make the scheme very promising for the generation of N -atom W -class states in spatially separated cavities.

II. THE MODEL

We consider N ($N \geq 3$) identical atoms trapped in N distant cavities which are connected by a single-mode integrated optical $1 \times N$ star coupler [29–31], as shown in Fig. 1(a). The optical star coupler is made up of N identical optical fiber channels and only one resonant

field mode interacts simultaneously with N cavity modes with a (real) coupling constant ν . Each atom is a two-level one playing the role of a qubit with $|0\rangle \equiv |g\rangle$, the ground state, and $|1\rangle \equiv |e\rangle$, the excited state. The atomic transition frequency Ω is detuned from the cavity mode frequency ω by a certain amount $\Delta = \Omega - \omega$, as shown in Fig. 1(b). Thus, the atomic transition $|g\rangle \leftrightarrow |e\rangle$ is dispersively coupled to the corresponding cavity mode with a (real) coupling constant f . The interaction Hamiltonian of the whole atom-cavity-fiber system under the rotating-wave approximation can be written as ($\hbar = 1$)

$$H = H_1 + H_2, \quad (1)$$

$$H_1 = \sum_{l=1}^N \nu (a_l^\dagger b + b^\dagger a_l), \quad (2)$$

$$H_2 = \sum_{l=1}^N f (a_l^\dagger S_l^- e^{-i\Delta t} + S_l^+ a_l e^{i\Delta t}), \quad (3)$$

where a_l^\dagger (a_l) is the creation (annihilation) operator of the l th cavity mode, b^\dagger (b) is the creation (annihilation) operator of the fiber mode and $S_l^+ = |e_l\rangle\langle g_l|$ ($S_l^- = |g_l\rangle\langle e_l|$) denotes the raising (lowering) operator of the l th atom.

We introduce new bosonic operators c_α defined by a linear superposition of a_l ($l = 1, 2, \dots, N$) and b

$$c_\alpha = \sum_{l=1}^N t_{\alpha,l} a_l + t_{\alpha,N+1} b, \quad (4)$$

where $t_{\alpha,\beta}$ with $\alpha, \beta \in \{1, 2, \dots, N+1\}$ are the elements of a $(N+1) \times (N+1)$ real unitary matrix T of the form

$$T = \begin{pmatrix} \frac{\sqrt{N-1}}{\sqrt{N}} & \frac{-1}{\sqrt{N(N-1)}} & \frac{-1}{\sqrt{N(N-1)}} & \cdots & \frac{-1}{\sqrt{N(N-1)}} & \frac{-1}{\sqrt{N(N-1)}} & \frac{-1}{\sqrt{N(N-1)}} & 0 \\ 0 & \frac{\sqrt{N-2}}{\sqrt{N-1}} & \frac{-1}{\sqrt{(N-1)(N-2)}} & \cdots & \frac{-1}{\sqrt{(N-1)(N-2)}} & \frac{-1}{\sqrt{(N-1)(N-2)}} & \frac{-1}{\sqrt{(N-1)(N-2)}} & 0 \\ 0 & 0 & \frac{\sqrt{N-3}}{\sqrt{N-2}} & \cdots & \frac{-1}{\sqrt{(N-2)(N-3)}} & \frac{-1}{\sqrt{(N-2)(N-3)}} & \frac{-1}{\sqrt{(N-2)(N-3)}} & 0 \\ \vdots & \vdots & \vdots & \ddots & \vdots & \vdots & \vdots & \vdots \\ 0 & 0 & 0 & \cdots & \frac{\sqrt{2}}{\sqrt{3}} & \frac{-1}{\sqrt{3 \times 2}} & \frac{-1}{\sqrt{3 \times 2}} & 0 \\ 0 & 0 & 0 & \cdots & 0 & \frac{1}{\sqrt{2}} & \frac{-1}{\sqrt{2 \times 1}} & 0 \\ \frac{-1}{\sqrt{2N}} & \frac{-1}{\sqrt{2N}} & \frac{-1}{\sqrt{2N}} & \cdots & \frac{-1}{\sqrt{2N}} & \frac{-1}{\sqrt{2N}} & \frac{-1}{\sqrt{2N}} & \frac{1}{\sqrt{2}} \\ \frac{1}{\sqrt{2N}} & \frac{1}{\sqrt{2N}} & \frac{1}{\sqrt{2N}} & \cdots & \frac{1}{\sqrt{2N}} & \frac{1}{\sqrt{2N}} & \frac{1}{\sqrt{2N}} & \frac{1}{\sqrt{2}} \end{pmatrix}. \quad (5)$$

The inverse transformations of Eq. (4) are

$$a_l = \sum_{\alpha=1}^{N+1} \chi_{l,\alpha} c_\alpha, \quad (6)$$

$$b = \sum_{\alpha=1}^{N+1} \chi_{N+1,\alpha} c_\alpha, \quad (7)$$

where $\chi_{\alpha,\beta}$ are the elements of a $(N+1) \times (N+1)$ real unitary matrix

$$X = T^{-1} = T^T. \quad (8)$$

In terms of the new delocalized bosonic operators in Eq. (4), H_1 and H_2 read

$$H_1 = -\sqrt{N}\nu \left(c_N^\dagger c_N - c_{N+1}^\dagger c_{N+1} \right) \quad (9)$$

and

$$H_2 = \sum_{l=1}^N \sum_{\alpha=1}^{N+1} f \chi_{l,\alpha} \left(S_l^+ c_\alpha e^{i\Delta t} + c_\alpha^\dagger S_l^- e^{-i\Delta t} \right). \quad (10)$$

Switching to the interaction representation, $\mathcal{H} = \mathcal{H}_0 + \mathcal{H}_{int}$, with $\mathcal{H}_0 = H_1$, we have

$$\mathcal{H}_{int} = \sum_{l=1}^N \sum_{\alpha=1}^{N+1} f \chi_{l,\alpha} \left(S_l^+ c_\alpha e^{i\Delta_\alpha t} + c_\alpha^\dagger S_l^- e^{-i\Delta_\alpha t} \right), \quad (11)$$

where

$$\Delta_\alpha = \begin{cases} \Delta & \text{for } \alpha = 1, 2, \dots, N-1 \\ \Delta + \sqrt{N}\nu & \text{for } \alpha = N \\ \Delta - \sqrt{N}\nu & \text{for } \alpha = N+1 \end{cases}. \quad (12)$$

We assume that all the cavities and the fibers are empty and only one atom is excited initially. Then, in the large detuning regime: $\Delta, |\Delta \pm \sqrt{N}\nu| \gg f$, the atoms are forbidden to exchange energy with the bosonic fields, but they can exchange energy with each other via virtual field modes. So during the system's evolution no real bosonic modes appear at all, but the atomic excitation can still propagate from atom to atom. The underlying dynamics is thus governed by the effective interaction Hamiltonian

$$\mathcal{H}_{eff} = \sum_{l,m=1}^N \xi_{lm} S_l^+ S_m^-, \quad (13)$$

with

$$\xi_{lm} = f^2 \sum_{\alpha=1}^{N+1} \frac{\chi_{l,\alpha} \chi_{m,\alpha}}{\Delta_\alpha}. \quad (14)$$

Using the equalities $\chi_{l,\alpha} = t_{\alpha,l}$ due to Eq. (8), the unitarity of $T : \sum_{\alpha=1}^{N+1} t_{\alpha,\beta} t_{\alpha,\delta} = \delta_{\beta\delta}$, and the properties $-t_{N,\beta} = t_{N+1,\beta} = 1/\sqrt{2N}$ for $\beta \in \{1, 2, \dots, N\}$, we can verify that

$$\xi_{lm} = \begin{cases} \frac{f^2}{N} \left(\frac{N-1}{\Delta} + \frac{\Delta}{\Delta^2 - N\nu^2} \right) = \xi_N & \text{for } l = m \\ -\frac{f^2}{N} \left(\frac{1}{\Delta} - \frac{\Delta}{\Delta^2 - N\nu^2} \right) = -\eta_N & \text{for } l \neq m \end{cases}. \quad (15)$$

Now we turn to the generation of N -atom W -class states via the effective interaction Hamiltonian in Eq. (13). In the subspace having only one excited atom and no real bosonic modes, the atoms' state at any time t can be represented by a linear superposition of N basic states $\{|\phi_n\rangle; n = 1, 2, \dots, N\}$ as

$$|\Phi_N(t)\rangle = \sum_{n=1}^N C_n^{(N)}(t) |\phi_n\rangle, \quad (16)$$

where $|\phi_n\rangle = |\dots e_n \dots\rangle$ denotes a state in which only the n th atom is excited while all the other $N - 1$ atoms are in their ground states. From the equation of motion $i\partial |\Phi_N(t)\rangle / \partial t = \mathcal{H}_{eff} |\Phi_N(t)\rangle$, the time-dependent coefficients $C_n^{(N)}(t)$ must satisfy the differential equations

$$i \frac{\partial C_n^{(N)}(t)}{\partial t} = \xi_N C_n^{(N)}(t) - \eta_N \sum_{l=1; l \neq n}^N C_l^{(N)}(t) \quad (17)$$

for $n = 1, 2, \dots, N$. Without loss of generality, we assume that at $t = 0$ the atoms are in the state $|\phi_1\rangle = |e_1 g_2 \dots g_N\rangle$ [i.e., under the initial conditions $C_1^{(N)}(0) = 1$, $C_2^{(N)}(0) = C_3^{(N)}(0) = \dots = C_N^{(N)}(0) = 0$]. Then, the solution of Eqs. (17) can be found in the form

$$C_1^{(N)}(t) = \frac{1}{N} e^{-i(\xi_N + \eta_N)t} (e^{iN\eta_N t} + N - 1), \quad (18)$$

$$C_2^{(N)}(t) = C_3^{(N)}(t) = \dots = C_N^{(N)}(t) = \frac{1}{N} e^{-i(\xi_N + \eta_N)t} (e^{iN\eta_N t} - 1). \quad (19)$$

As is evident from Eqs. (18) and (19), at $t \neq \frac{2k\pi}{N\eta_N}$ ($k = 0, 1, 2, \dots$) all the coefficients $C_n^{(N)}(t) \neq 0$ ($n = 1, 2, \dots, N$) and thus the state $|\Phi_N(t)\rangle$ of Eq. (16) is an N -atom W -class state. In particular, omitting an unimportant common phase factor, states of the form

$$|\Psi_N\rangle = \frac{1}{N} [(N-2)|\phi_1\rangle - 2 \sum_{n=2}^N |\phi_n\rangle] \quad (20)$$

are generated at

$$t = \frac{(2k+1)\pi}{N\eta_N}. \quad (21)$$

III. NUMERICAL ANALYSIS

In order to verify the validity of the above theoretical result, we analyze the system's dynamics by numerically solving the Schrödinger equation with the full Hamiltonian H in Eq. (1). Suppose that we aim at generating the N -atom W -class state $|\Psi_N\rangle$ given in Eq. (20). In Fig. 2 we plot the fidelity $F_N = \langle \Psi_N | \rho_N(t) | \Psi_N \rangle$ of the atoms' state $\rho_N(t)$ obtained from the numerical calculation with respect to the state $|\Psi_N\rangle$ for various values of N and the parameters chosen as $\Delta/f = \nu/f = 10$. Figure 2(a) shows F_N versus dimensionless time $\tau = N\eta_N t$, showing that $F_N \simeq 1$ at $\tau = (2k+1)\pi$ for any N which is in agreement with the theoretical result of Eq. (21). Alternatively, we also plot F_N versus another dimensionless time ft in Fig. 2(b), from which it follows that the time for F_N to reach 1 is longer if N is larger. This also agrees with the theoretical result of Eq. (21), because $N\eta_N$, with η_N defined by Eq. (15), decreases with increasing N . The slow oscillation of F_N in Fig. 2 is due to the “hopping” of atomic excitation among the atoms due to the virtual excitation of the field modes, as theoretically predicted by Eqs. (18) and (19) when the effective Hamiltonian (13) is used. As for the fast oscillation in the fidelity F_N , it results from the atom-cavity energy exchange based on the use of the full Hamiltonian (1).

To be more concrete, let us deal with a specific situation for $N = 4$ and $t = \pi/4\eta_4$, i.e., the target W -class state is

$$|\Psi_4\rangle = \frac{1}{2}(|e_1g_2g_3g_4\rangle - |g_1e_2g_3g_4\rangle - |g_1g_2e_3g_4\rangle - |g_1g_2g_3e_4\rangle). \quad (22)$$

It is necessary to consider the influence of different detunings on the fidelity $F_4 = \langle \Psi_4 | \rho_4(t) | \Psi_4 \rangle$. For $N = 4$, the condition $\Delta/\nu < 2$ should be satisfied according to Eq. (21). Thus, we assume ν and Δ such that $\nu = 10f$ and $2f < \Delta < 12f$ for plotting the fidelity F_4 against different Δ in Fig. 3, where the oscillatory behavior is mainly caused by the energy exchange between the atoms and the fields. The numerical result shows that the average fidelity becomes closer to 1 for a larger detuning Δ . That is, a larger detuning suits the scheme better under an ideal environment. However, a quantum system interacts with the noisy environment inevitably, which induces unwanted disturbance to the target entangled state. The decoherence originates from physical factors such as the atomic spontaneous emission, the cavity decay and the fiber decay. To account for these decoherence factors, we employ the master equation for the density matrix ρ of the whole system, which is of the

well-known form

$$\begin{aligned}
\dot{\rho} = & -i[H, \rho] - \sum_{l=1}^N \frac{\Gamma_l}{2} (S_l^+ S_l^- \rho - 2S_l^- \rho S_l^+ + \rho S_l^+ S_l^-) \\
& - \sum_{l=1}^N \frac{\gamma_l}{2} (a_l^\dagger a_l \rho - 2a_l \rho a_l^\dagger + \rho a_l^\dagger a_l) \\
& - \frac{\kappa}{2} (b^\dagger b \rho - 2b \rho b^\dagger + \rho b^\dagger b),
\end{aligned} \tag{23}$$

where Γ_l is the spontaneous emission rate from the excited state $|e\rangle$ to the ground state $|g\rangle$ of the l th atom, γ_l is the decay rate of the l th cavity and κ is the decay rate of the optical star coupler. Assuming $\Gamma_l = \Gamma$ and $\gamma_l = \gamma$ for simplicity, the dependence of the fidelity F_4 on Δ/f and Δ/ν in Fig. 4 can be obtained by numerically solving the master equation (23). For $0.8 < \Delta/\nu < 2$ and Δ/f being a constant, we find that the fidelity decreases quickly when $\Delta/\nu \rightarrow 2$, in which case the large detuning condition $|\Delta - \sqrt{4}\nu| \gg f$ is not satisfied. This implies that use of the effective Hamiltonian in Eq. (13) is not valid in this case. With the decreasing of Δ/ν , the large detuning condition is getting satisfied and the dynamics of the whole system will evolve in accordance with that governed by the effective Hamiltonian. As seen from Fig. 4(a), the fidelity drops slowly when $\Delta/\nu \leq 1$ and $\Gamma/f = 0.01$. This is because the interaction time needed to achieve the target entangled state prolongs according to Eq. (21), causing more decoherence from atomic spontaneous emission since the probability of population in the atomic excited state is larger. The fidelity in Fig. 4(b) ((c)) keeps very high even when $\Delta/\nu \leq 1$ and $\gamma/f = 0.3$ ($\kappa/f = 0.3$), revealing robustness of the fidelity against the cavity decay and fiber decay due to the fact that the probabilities of real population in the cavity and the fiber are negligible in the effective Hamiltonian (13) that contains no interaction terms among those field modes. Keeping the ratio Δ/ν fixed in Fig. 4, we can consider the effect of different Δ on the fidelity. From Fig. 4, we can see that the increase of Δ will decrease the fidelity with an oscillatory behavior. This is because although Δ is large the interaction time prolongs with the increasing of Δ in accordance with Eq. (21), where the decoherence dominates the system dynamics. Therefore, the range $0.8 < \Delta/\nu < 1.2$ is the appropriate choice in our scheme. It also shows that the fidelity is robust against the possible imprecision of the atom-cavity detuning and the coupling strength between the bosonic modes.

Next, by choosing an appropriate values $\Delta/f = \nu/f = 10$ in Figs. 5(a) ((b)), we plot the fidelity versus the ratios Γ/f and γ/f (Γ/f and κ/f). These figures indicate that the

atomic spontaneous emission dominates the reduction of fidelity, while the decay rates of the photon leaking out off each cavity and the optical fiber channels just slightly influence F_4 , which is 0.93 (0.97) even when $\gamma/f = 0.3$ ($\kappa/f = 0.3$). Hence, the scheme is remarkably robust against cavity and fiber decays, which can be understood by the virtual excitation of all the bosonic field modes.

Finally, we briefly discuss the basic elements that may be a candidate for further experiments. The requirements of our scheme are the two-level atoms and the cavities resonantly connected by an optical fiber star coupler. The single-mode integrated optical fiber $1 \times N$ star coupler used as a distributed strain sensor in a white-light interferometer has been reported [31] and realized by using a 2D arrangement, by using the two confocal arrays of the radial waveguides which performs with an efficiency 100% under ideal conditions when the waveguides' mutual coupling strength is strong [32]. A near-perfect fiber-cavity coupling with an efficiency larger than 99.9% can be realized using fiber-taper coupling to high-Q silica microspheres [33]. The atomic configuration can be achieved with cesium: state $|g\rangle$ corresponds to $\{F = 4, m = 3\}$ hyperfine state of $6^2S_{1/2}$ electronic ground state and state $|e\rangle$ corresponds to $\{F = 4, m = 3\}$ hyperfine state of $6^2P_{1/2}$ electronic state. Each single atom can be made localized at a fixed position in each cavity with high Q for a long time [34–36]. In recent experiments [37, 38], the parameters $f = 2\pi \times 750$ MHz, $\Gamma = 2\pi \times 2.62$ MHz and $\gamma = 2\pi \times 3.5$ MHz with the wavelength in the region $630 \sim 850$ nm is predicted achievable. The optical fiber decay at a 852 nm wavelength is about 2.2 dB/km [39], which corresponds to fiber decay rate 0.152 MHz. By substituting these experimental parameters into Eq. (23), we obtain a fidelity higher than 0.9, making our scheme possible to be realized in experiment. The generation of W -class states involving more atoms is also efficient by changing the corresponding experimental parameters.

IV. CONCLUSION

We have considered a model consisting of any $N \geq 3$ identical two-level atoms trapped in N spatially separated cavities. Each cavity has one active mode which is off-resonant with the atomic transition but resonant with a single mode of an integrated optical $1 \times N$ star coupler (see Fig. 1), so all the atoms are indirectly coupled to each other even though they are far apart. We deduce an effective Hamiltonian in the large atom-cavity mode

detuning regime and use it to theoretically study the dynamics of the atoms' system under the initial condition that only one atom is excited while all the cavities and the fiber are empty. The theoretical result shows that as the system evolves the atoms generally appear in an N -atom W -class state. Of interest are the multiatom entangled states of the form in Eq. (20) which are generated periodically at time moments determined by Eq. (21). The proposed scheme for generating N -atom W -class states does not require any external classical laser pulses and is insensitive to the cavity decay rate and the rate of photon leakage from the fiber because during the whole evolution no real bosons are to be created due to the large detuning between the atomic transition and the cavity mode. We have also carried out numerical calculations taking into account the effects of decoherence caused by various dissipation mechanisms. The numerical result agrees well with the theoretical one if the atom-cavity detuning is large enough, confirming the validity of the effective Hamiltonian with respect to the full one. Therefore, the present entanglement generation scheme proves to be perspective for wide applications in the scalable distributed quantum networks.

V. ACKNOWLEDGMENTS

M. L and Y. X were supported by the National Natural Science Foundation of China under grant no. 11047122 and no. 11105030, and China Postdoctoral Science Foundation under grant no. 20100471450. N. B. A. was funded by Vietnam National Foundation for Science and Technology Development (NAFOSTED) under grant no. 103.99-2011.26.

-
- [1] H. J. Kimble, "The quantum internet," *Nature* **453**, 1023-1030 (2008).
 - [2] S. B. Zheng and G. C. Guo, "Efficient scheme for two-atom entanglement and quantum information processing in cavity QED," *Phys. Rev. Lett.* **85**, 2392 (2000).
 - [3] C. H. Bennett and G. Brassard, C. Crépeau, R. Jozsa, A. Peres and W. Wootters, "Teleporting an unknown quantum state via dual classical and Einstein-Podolsky-Rosen channels," *Phys. Rev. Lett.* **70**, 1895 (1993).
 - [4] C. H. Bennett and S. J. Wiesner, "Communication via one- and two-particle operators on Einstein-Podolsky-Rosen states," *Phys. Rev. Lett.* **69**, 2881 (1992).

- [5] A. K. Ekert, "Quantum cryptography based on Bell's theorem," *Phys. Rev. Lett.* **67**, 661 (1991).
- [6] D. Gottesman and I. Chuang, "Demonstrating the viability of universal quantum computation using teleportation and single-qubit operations," *Nature* **402**, 390-393 (1999).
- [7] J. S. Bell, *Phys.* "On the Einstein Podolsky Rosen Paradox," **1**, 195 (1964).
- [8] D. M. Greenberger, M. Horne, A. Shimony, and A. Zeilinger, "Bell's theorem without inequalities," *Am. J. Phys.* **58**, 1131 (1990).
- [9] Y. Xia, J. Song, and H. S. Song, "Linear optical protocol for preparation of N-photon Greenberger-Horne-Zeilinger state with conventional photon detectors," *Appl. Phys. Lett.* **92**, 021127 (2008).
- [10] W. Dür, G. Vidal, and J. I. Cirac, "Three qubits can be entangled in two inequivalent ways," *Phys. Rev. A* **62**, 062314 (2000).
- [11] H. J. Briegel and R. Raussendorf, "Persistent entanglement in arrays of interacting particles," *Phys. Rev. Lett.* **86**, 910 (2001).
- [12] J. Joo, Y. J. Park, S. Oh, and J. Kim, "Quantum teleportation via a W state," *New J. Phys.* **5**, 136 (2003).
- [13] P. Agrawal and A. Pati, "Perfect teleportation and superdense coding with W states," *Phys. Rev. A* **74**, 062320 (2006).
- [14] S. B. Zheng, "Splitting quantum information via W states," *Phys. Rev. A* **74**, 054303 (2006).
- [15] H. Z. Wu, Z. B. Yang, W. J. Su, Z. R. Zhong, and J. M. Huang, "Quantum information splitting based on current cavity QED techniques," *Commun. Theor. Phys.* **49**, 1165 (2008).
- [16] W. Cui, E. Chitambar, and H. Kwong. Lo, "Optimal entanglement transformations among N-qubit W-class states," *Phys. Rev. A* **82**, 062314 (2010).
- [17] T. Bastin, C. Thiel, J. von Zanthier, L. Lamata, E. Solano, and G. S. Agarwal, "Operational determination of multiqubit entanglement classes via tuning of local operations," *Phys. Rev. Lett.* **102**, 053601 (2009).
- [18] N. B. An, "Cavity-catalyzed deterministic generation of maximal entanglement between non-identical atoms," *Phys. Lett. A* **344**, 77 (2005).
- [19] X. W. Wang, G. J. Yang, Y. H. Su, and M. Xie, "Simple schemes for quantum information processing with W-type entanglement," *Quant. Info. Proc.* **8**, 431 (2009).
- [20] T. Pellizzari, "Quantum networking with optical fibres," *Phys. Rev. Lett.* **79**, 5242 (1997)

- [21] A. Serafini, S. Mancini, and S. Bose, “Distributed quantum computation via optical fibers,” *Phys. Rev. Lett.* **96**, 010503 (2006).
- [22] J. Song, Y. Xia, H. S. Song, J. L. Guo, and J. Nie, “Quantum computation and entangled-state generation through adiabatic evolution in two distant cavities,” *Eur. Phys. Lett.* **80**, 60001 (2007).
- [23] J. Song, Y. Xia, and H. S. Song, “Quantum nodes for W-state generation in noisy channels,” *Phys. Rev. A* **78**, 024302 (2008).
- [24] S. B. Zheng, C. P. Yang, and F. Nori, “Arbitrary control of coherent dynamics for distant qubits in a quantum network,” *Phys. Rev. A* **82**, 042327 (2010).
- [25] Z. Q. Yin and F. L. Li, “Multiatom and resonant interaction scheme for quantum state transfer and logical gates between two remote cavities via an optical fiber,” *Phys. Rev. A* **75**, 012324 (2007).
- [26] X. Y. Lü, L. G. Si, X. Y. Hao, and X. Yang, “Achieving multipartite entanglement of distant atoms through selective photon emission and absorption processes,” *Phys. Rev. A* **79**, 052330 (2009).
- [27] L. T. Shen, H. Z. Wu, and Z. B. Yang, “Distributed phase-covariant cloning with atomic ensembles via quantum Zeno dynamics,” *Eur. Phys. J. D* **66**, 123 (2012).
- [28] A. Sen(De), U. Sen, M. Wiśniak, D. Kaszlikowski, and M. Żukowski, “Multiqubit W states lead to stronger nonclassicality than Greenberger-Horne-Zeilinger states,” *Phys. Rev. A* **68**, 062306 (2003).
- [29] T. Findakly and B. Chen, “Single-mode integrated optical $1\times N$ star coupler,” *Appl. Phys. Lett.* **40**, 549 (1982).
- [30] H. Feng, E. H. Li, and K. Tada, “Analysis of X-intersecting waveguide switches with a large branching angles ranging from 2° to 12° ,” *Jpn. J. Appl. Phys.* **36**, 5136 (1997).
- [31] L. B. Yuan and L. M. Zhou, “ $1\times N$ star coupler as a distributed fiber-optic strain sensor in a white-light interferometer,” *Appl. Opt.* **37**, 4168 (1998).
- [32] C. Dragone, C. H. Henry, I. P. Kaminow, and R. C. Kistler, “Efficient multichannel integrated optics star coupler on silicon,” *IEEE Photon. Technol. Lett.* **1**, 241 (1989).
- [33] K. J. Gordon, V. Fernandez, P. D. Townsend, and G. S. Buller, “A short wavelength GigaHertz clocked fiber-optic quantum key distribution system,” *IEEE J. Quantum Electron.* **40**, 900-908 (2004).

- [34] A. B. Mundt, A. Kreuter, C. Becher, D. Leibfried, J. Eschner, F. Schmidt-Kaler, and R. Blatt, “Coupling a single atomic quantum bit to a high finesse optical cavity,” *Phys. Rev. Lett.* **89**, 103001 (2002).
- [35] S. M. Spillane, T. J. Kippenberg, and K. J. Vahala, “Ultrahigh-Q toroidal microresonators for cavity quantum electrodynamics,” *Phys. Rev. A* **71**, 013817 (2005).
- [36] S. Osnaghi, P. Bertet, A. Auffeves, P. Maioli, M. Brune, J. M. Raimond, and S. Haroche, “Coherent control of an atomic collision in a cavity,” *Phys. Rev. Lett.* **87**, 037902 (2001).
- [37] S. M. Spillane, T. J. Kippenberg, K. J. Vahala, K. W. Goh, E. Wilcut, and H. J. Kimble, “Ultrahigh-Q toroidal microresonators for cavity quantum electrodynamics,” *Phys. Rev. A* **71**, 013817 (2005).
- [38] J. R. Buck and H. J. Kimble, “Optimal sizes of dielectric microspheres for cavity QED with strong coupling,” *Phys. Rev. A* **67**, 033806 (2003).
- [39] F. Dimer, B. Estienne, A. S. Parkins, and H. J. Carmichael, “Proposed realization of the Dicke-model quantum phase transition in an optical cavity QED system,” *Phys. Rev. A* **75**, 013804 (2007).

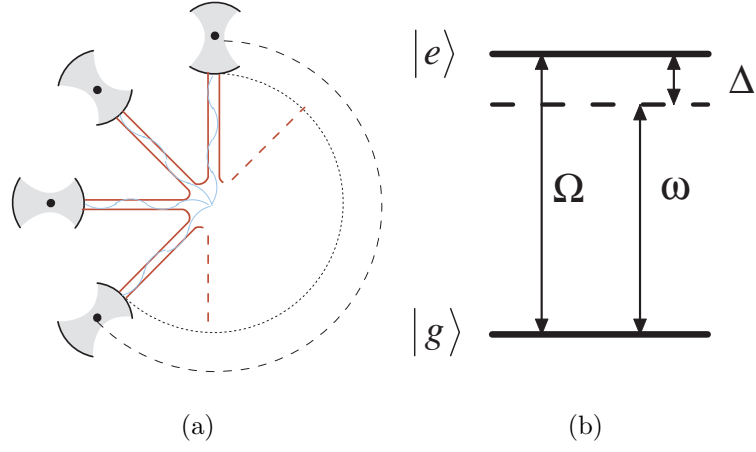
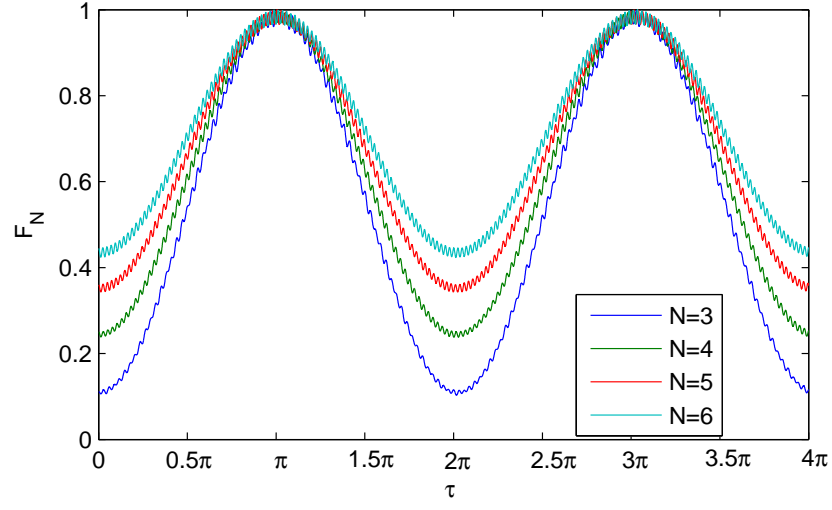
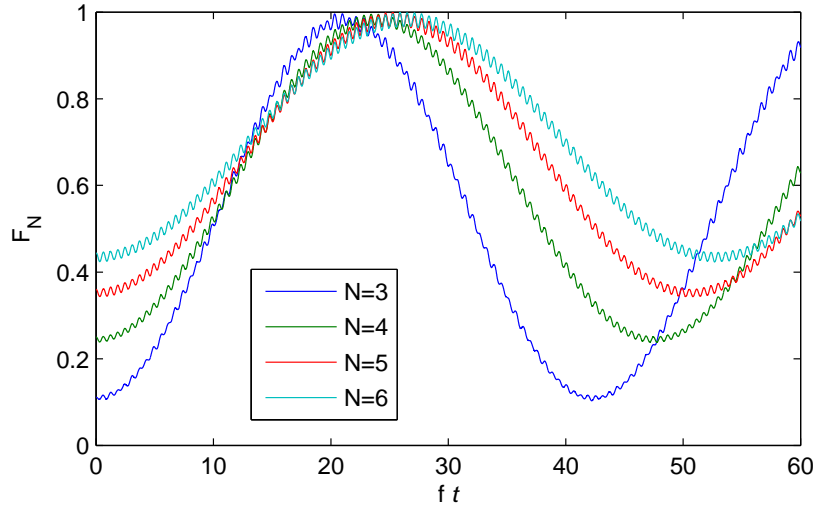


FIG. 1: (color online) (a) Experimental setup. The block dots denote the atoms, which are trapped in N distant cavities, and these cavities are connected by a $1 \times N$ single-mode integrated optical star coupler. (b) Level configuration for each atom.



(a)



(b)

FIG. 2: (color online) The fidelity F_N versus dimensionless time (a) $\tau = N\eta_N t$ and (b) ft , with $\Delta/f = \Delta/\nu = 10$ for $N = 3, 4, 5$ and 6 .

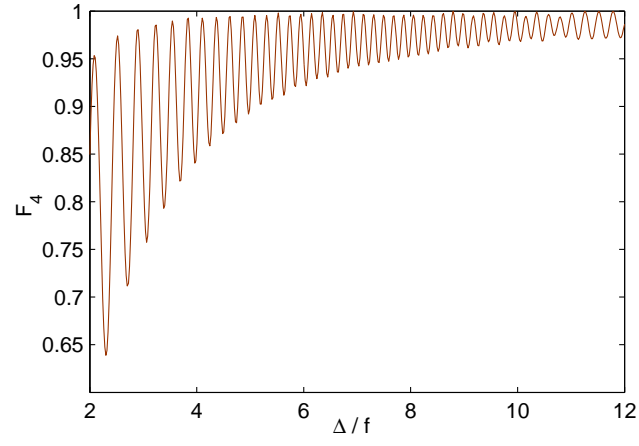
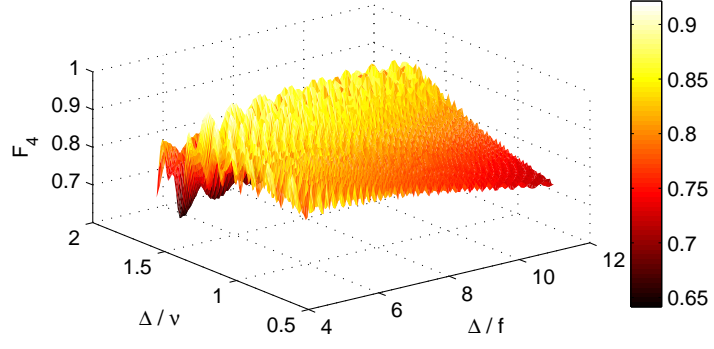
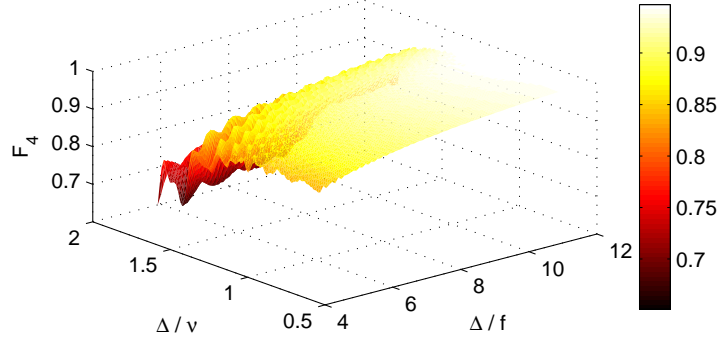


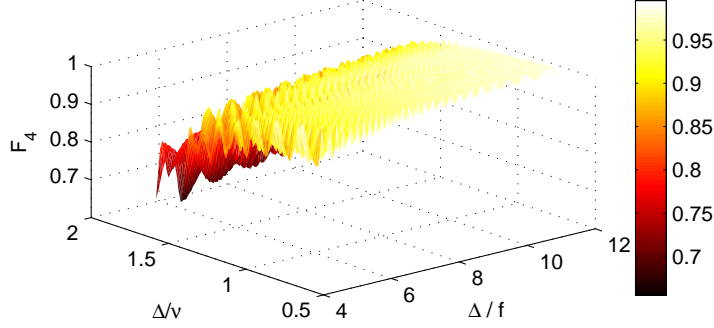
FIG. 3: (color online) The fidelity F_4 at $t = \pi/4\eta_4$ versus Δ/f when $\nu/f = 10$.



(a)



(b)



(c)

FIG. 4: (color online) The fidelity F_4 at $t = \pi/4\eta_4$ versus Δ/f and Δ/ν when (a) $\Gamma/f = 0.01$ and $\gamma = \kappa = 0$; (b) $\Gamma = \kappa = 0$ and $\gamma/f = 0.3$ and, (c) $\Gamma = \gamma = 0$ and $\kappa/f = 0.3$.

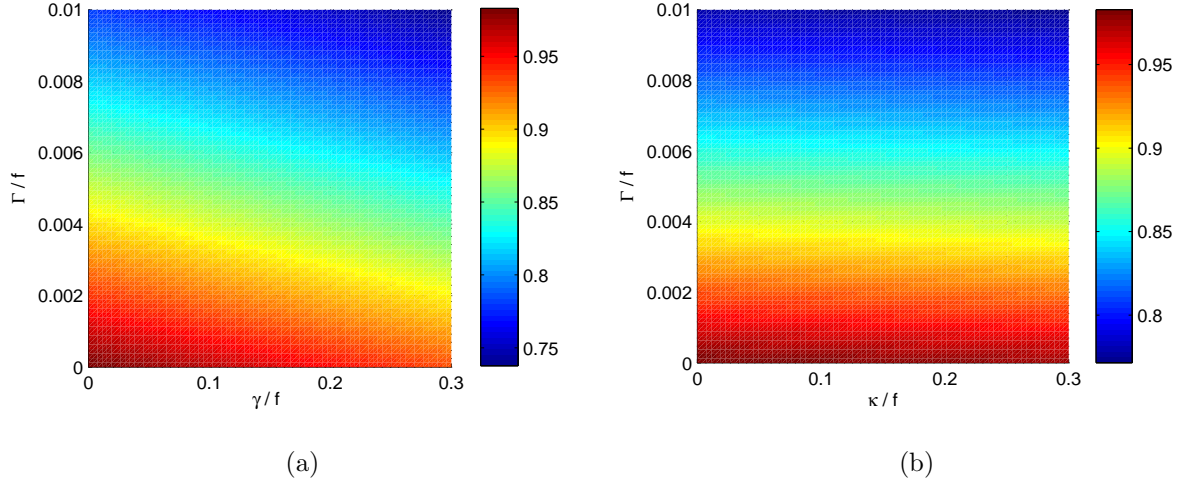


FIG. 5: (color online) Density plots of the fidelity F_4 at $t = \pi/4\eta_4$ versus (a) Γ/f and γ/f and (b) Γ/f and κ/f .